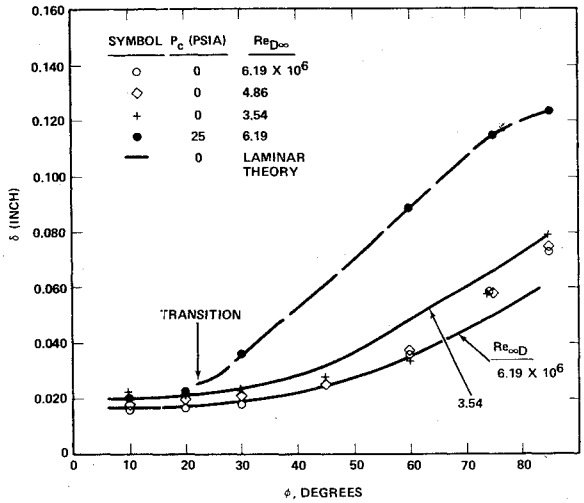

Fig. 2 Boundary-layer growth with and without injection.

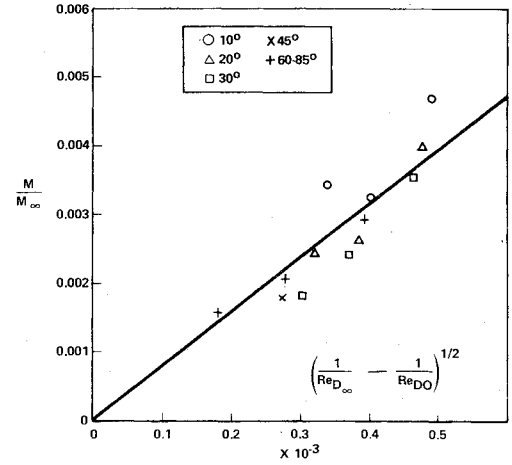

Fig. 3 Relation between the integrated mass flow, the resulting location of transition (in degrees from the stagnation point) and the hemisphere Reynolds number $Re_{\infty D}$.

layer thickness δ was close to the theoretical prediction, as shown on Fig. 2. Although a precise assessment of the measurement error in these profiles was not made, it was concluded that the theoretical predictions of laminar boundary-layer growth are satisfactory as represented in modern computer codes.[1]

When the mass addition rate exceeded a certain threshold at each flow Reynolds number, the boundary-layer became turbulent. This was evidenced not only by the profile changes and boundary-layer thickening (see Figs. 1 and 2) but most strikingly by the turbulence detected by the hot wire anemometers. From such data the transition location could be correlated by

$$\varphi_T = 893\left[\frac{1}{Re_{D_\infty}} - \left(\frac{1}{S}\frac{\dot{M}}{\dot{M}_\infty}\right)^2\right] 10^6 - 30(\text{degrees}) \qquad (2)$$

with

$$\dot{M}_\infty = \frac{\pi D^2}{4}\rho_\infty u_\infty \text{ (subtended mass flow)}$$

$$\dot{M} = \int_A \dot{m}\,dA \text{ (total mass flow rate ejected)} \qquad (3)$$

Implicit in this criterion is a data "correlation" for smooth, adiabatic hemispheres without mass addition which relates the angular transition location to the hemisphere Reynolds number as follows

$$\frac{1}{Re_{D_{\infty}(\dot{M}=0)}} = (0.036 + 0.00112\varphi) + 10^{-6} \quad (\varphi \text{ in degrees}) \qquad (4)$$

It should be stressed that this correlation is used here only as an approximation for the nonblowing limit and does not address subtle questions such as the effect of unit Reynolds number and freestream turbulence.

A linear least squares computer fit of all the data in Fig. 3 showed that the constant $S = 8.0$, as represented by the slope of the straight line on that figure. Slightly better agreement can be achieved if individual curve fits for each angle φ are performed, in which cases S varies from about 7 to about 9.

Theoretical considerations lead to the belief that mass addition increases the laminar boundary-layer thickness and simultaneously introduces changes in the velocity profile. By computing the increase in the momentum thickness Reynolds number Re_θ caused by the small but discernible thickening of the pretransitional layer (Fig. 2) it was tentatively concluded that the observed acceleration of transition with blowing could be explained in terms of this thickening alone. It is a much more difficult task to discern small velocity profile changes from the recorded data; this would of course, be a crucial step in predicting the observed transition results from the viewpoint of hydrodynamic stability.

A second important conclusion drawn from Figs. 1 and 2 is that the mass addition rates needed to cause transition are small. The mass addition parameter

$$|f_w(\varphi)| \equiv \frac{(\rho v)_w}{(2\rho_e\beta_e\mu_e)^{1/2}} \qquad (5)$$

was found to be at most of order 1. Theoretical efforts to predict "massive blowing" effects are based on laminar flow theory with f_w of order 10 or higher.[2] Therefore, it appears that, since the laminar boundary layer cannot support these large injection rates, the laminar flow computations dealing with such large rates should be reformulated to include the effect of turbulent mixing in the boundary layer.

References

[1] Bywater, R., Aerospace Corp., Los Angeles, Calif., private communications 1974-1975.

[2] Libby, P. A., "The Homogeneous Boundary Layer At An Axisymmetric Stagnation Point With Large Rates of Injection," *Journal of the Aeronautical Sciences*, Vol. 29, Jan. 1962, p. 48.

Statistical Analysis of Trim Maneuvers in Low-Thrust Interplanetary Navigation

George C. Rinker,* Robert A. Jacobson,†
Jet Propulsion Laboratory, Pasadena, Calif.
and
Lincoln J. Wood‡
Hughes Aircraft Company, El Segundo, Calif.

I. Introduction

ONE of the proposed applications of solar electric propulsion is the exploration of comets and asteroids. In order to effectively employ solar electric propulsion in flights to these bodies, difficult navigation problems must be over-

Presented as Paper 75-85 at the AIAA 13th Aerospace Sciences Meeting, Pasadena, Calif., January 20-22, 1975; submitted February 24, 1975; revision received December 22, 1975. This paper presents the results of one phase of research carried out at the Jet Propulsion Laboratory, California Institute of Technology, under contract NAS7-100, sponsored by NASA.

Index categories: Navigation, Control, and Guidance Theory; Spacecraft Navigation, Guidance, and Flight-Path Control Systems.

*Engineer, Mission Analysis Division. Associate Member AIAA.

†Senior Engineer, Mission Analysis Division. Member AIAA.

‡Staff Engineer. Formerly Bechtel Instructor in Engineering, California Institute of Technology, and Consultant, Jet Propulsion Laboratory. Member AIAA.

come. The primary obstacle to successful navigation is the nongravitational acceleration experienced by the vehicle as a result of random fluctuations in the thrust vector.[1-3]

Analysis of a 1980 Comet Encke slow flyby mission has indicated that a straightforward approach to solar electric propulsion terminal navigation will not provide the delivery accuracy necessary for effective scientific observations.[3-5] However, a strategy proposed in Ref. 5 lessens the problem of thrust vector errors and, consequently, permits successful terminal navigation. This strategy employs a navigation coast followed by a brief low-thrust trim maneuver. The absence of the thrust vector error source during the coast leads to improved orbit determination. The brief maneuver then corrects detected errors while minimizing thrust vector induced disturbances.

In order to effectively utilize the coast strategy, an optimum selection of coast and maneuver durations must be made. In Ref. 5, this selection is made by means of a parametric study of coast and maneuver durations using a linear perturbation guidance technique. Such a procedure is costly and inefficient; furthermore, linear perturbation guidance employs assumptions which do not strictly apply to the coast strategy as it would be implemented in mission operations. In order to use linear perturbation guidance, it must be assumed that a maneuver is nominally scheduled and that trajectory corrections are made with small adjustments of that maneuver. In the proposed coast arc strategy no nominal maneuver exists, and the trim is viewed as a maneuver inserted into the coast solely for navigation. Moreover, the trim maneuver utilizes the entire thrust vector for trajectory correction, not just a small portion as in linear perturbation guidance. Consequently, if the coast navigation strategy is to be considered in future analysis of low-thrust missions, an alternative to the linear analysis method is needed.

In this paper we present an analytical technique for determining the statistical properties of the trim maneuver when given the thrust available and the state dispersion and orbit determination covariances at the maneuver time. Also included is a procedure for mapping the covariances through the maneuver with execution errors taken into account. The analytical results are applied to a 1980 solar electric propulsion Encke flyby mission.

II. Analytical Formulation

Guidance Strategy

Let $\delta r(t)$ and $\delta V(t)$ denote perturbations in the spacecraft's position and velocity relative to the nominal trajectory at time t, and let $\delta\hat{r}(t)$ and $\delta\hat{V}(t)$ represent estimates of these perturbations. The initiation time of the trim maneuver, its termination time, and the time of encounter are denoted by t_0, t_1, and t_2, respectively. If the thrust acceleration is roughly tant during the maneuver, and if the maneuver duration is substantially less than the characteristic times of Φ_{12}, then

$$\delta\hat{r}(t_2) \simeq \Phi_{11}(t_2,t_0)\delta\hat{r}(t_0) + \Phi_{12}(t_2,t_0)\delta\hat{V}(t_0) + \Phi_{12}(t_2,t_0)u\Delta t \tag{1}$$

where Φ_{11} and Φ_{12} are transition matrices, u is the thrust acceleration, and $\Delta t = t_1 - t_0$. Equation (1) may be written in impact plane coordinates (the impact plane is the plane normal to the nominal spacecraft-target relative velocity vector at encounter) as

$$F y + \hat{z} = R\delta\hat{r}(t_2) \tag{2}$$

where R is the orthogonal transformation matrix from heliocentric to impact plane coordinates and

$$\hat{z} = R[\Phi_{11}(t_2,t_0)\delta\hat{r}(t_0) + \Phi_{12}(t_2,t_0)\delta\hat{V}(t_0)] \tag{3}$$

$$y = R\,u\Delta t \tag{4}$$

$$F = R\Phi_{12}(t_2,t_0)R^T \tag{5}$$

The objective of the guidance scheme is to null the expected crosstrack and out-of-plane position errors at encounter while minimizing maneuver duration. If the interval between the trim maneuver and encounter is small compared to the orbital period, the guidance objective may be accomplished by a control law in which y_1 is set to zero, and y_2 and y_3 are used to control the encounter position errors. Such a control law is

$$y = -A\hat{z} \tag{6}$$

where

$$A = (F_{22}F_{33} - F_{32}F_{23})^{-1} \begin{bmatrix} 0 & 0 & 0 \\ 0 & F_{33} & -F_{23} \\ 0 & -F_{32} & F_{22} \end{bmatrix} \tag{7}$$

The subscripts 1, 2, and 3 denote downtrack, crosstrack, and out-of-plane vector components.

Statistical Properties of the Maneuver

The estimated spacecraft state perturbation vector $\hat{x}(t_0)$

$$\left(\hat{x}^T(t_0) = [\delta\hat{r}^T(t_0),\ \delta\hat{V}^T(t_0)]\right)$$

is assumed to be a gaussian random vector with zero mean and covariance $\hat{X}(t_0)$. It follows then that the covariance $\bar{Y}$ of y is

$$\bar{Y} = A\,R\,[\Phi_{11}\ \Phi_{12}]\,\hat{X}\begin{bmatrix} \Phi_{11}^T \\ \Phi_{12}^T \end{bmatrix} R^T A^T \tag{8}$$

By design, the first component of y is always zero, so the first row and column of $\bar{Y}$ are identically zero. The joint probability density function of y_2 and y_3 is

$$p(y_2,y_3) = \frac{1}{2\pi}\,|Y|^{-1/2} \exp\left\{-\tfrac{1}{2}[y_2,y_3]\,Y^{-1} \times \begin{bmatrix} y_2 \\ y_3 \end{bmatrix}\right\} \tag{9}$$

where Y is the lower right 2×2 partition of $\bar{Y}$.

The duration of the trim maneuver is

$$\Delta t = \frac{|y|}{u} \tag{10}$$

The joint probability density function of Δt and θ, the thrust direction angle in the impact plane, follows from Eq. (9)

$$p(\Delta t,\theta) = \frac{\alpha_3\Delta t}{2\pi}\,e^{-(\Delta t)^2(\alpha_1+\alpha_2\cos 2\theta)} \tag{11}$$

for $\Delta t \geq 0$, where

$$\alpha_1 = \frac{\lambda_1+\lambda_2}{4\lambda_1\lambda_2}\,u^2,\quad \alpha_2 = \frac{\lambda_2-\lambda_1}{4\lambda_1\lambda_2}\,u^2,\quad \alpha_3 = \frac{u^2}{(\lambda_1\lambda_2)^{1/2}} \tag{12}$$

λ_1 and λ_2 are the eigenvalues of Y, and θ is measured from the eigenvector direction corresponding to λ_1. The marginal probability density functions of Δt and θ, obtained from Eq. (11), are

$$p(\Delta t) = \alpha_3\Delta t\,e^{-\alpha_1(\Delta t)^2} I_0(\alpha_2(\Delta t)^2) \tag{13}$$

$$p(\theta) = \frac{\alpha_3}{4\pi}\,(\alpha_1+\alpha_2\cos 2\theta)^{-1} \tag{14}$$

where I_0 is the zero-order modified Bessel function of the first kind.

Although Δt is nongaussian, it is of some interest to know its first two moments, the mean and variance. These may be computed directly from the marginal density function (13)

$$\overline{\Delta t} = \left(\frac{2\lambda_2}{\pi}\right)^{1/2}\frac{1}{u}\,E\left[\left(1-\frac{\lambda_1}{\lambda_2}\right)^{1/2}\right] \quad \text{for } \lambda_2 \geq \lambda_1 \tag{15}$$

$$\sigma^2_{\Delta t} = \frac{\lambda_1+\lambda_2}{u^2} - (\overline{\Delta t})^2 \tag{16}$$

where $E[\cdot]$ is the complete elliptic integral of the second kind. The probability distribution function of Δt, i.e., the probability that the maneuver duration is less than Δt, can also be determined in principle from Eq. (13). However, no closed form expression for the function appears obtainable. By utilizing the Maclaurin series representation of I_0, the following series expansion can be formed for the distribution function $G(\Delta t)$

$$G(\Delta t) = 1 - \frac{\alpha_3}{2\alpha_1}\,e^{-\alpha_1(\Delta t)^2}\sum_{n=0}^{\infty}\left[\frac{(\alpha_2/\alpha_1)^{2n}}{2^{2n}(n!)^2}\,(2n)!\times\sum_{r=0}^{2n}\frac{(\alpha_1(\Delta t)^2)^r}{r!}\right] \tag{17}$$

The properties of Δt are similar to the statistical properties presented by Lee and Boain[6] for the magnitude of the velocity change $|\Delta V|$ during a midcourse maneuver in a ballistic mission. However, their expression for the mean of $|\Delta V|$ is more complicated than Eq. (15) and more difficult to evaluate, since it involves a hypergeometric function rather than an elliptic integral. A detailed derivation of Eq. (15) appears in Ref. 7.

Table 1 Knowledge and delivery errors before and after the trim maneuver

Navigation coast	Knowledge before	Delivery before	Knowledge/ delivery after
Length (days)	SMAA (km)	SMAA (km)	SMAA (km)
0	747	1703	764
2	441	1580	470
4	415	1595	444
7	409	1683	440
10	408	2444	477

Propagation of the Covariance Matrices Through the Trim Maneuver

Under the assumption that the state estimate and the error in the estimate are uncorrelated, the state covariance X and the covariance of the error in the state estimate P, satisfy

$$X = \hat{X} + P \tag{18}$$

Propagation of X through the maneuver is accomplished by propagating $\hat{X}$ and P. The estimated state perturbations after the trim maneuver are given approximately by

$$\hat{x}(t_1) \approx \tilde{A}\hat{x}(t_0) \tag{19}$$

where

$$\tilde{A} = \left[\begin{array}{c|c} I & 0 \\ \hline -R^T A R \Phi_{11}(t_2,t_0) & I - R^T A R \Phi_{12}(t_2,t_0) \end{array}\right] \tag{20}$$

and the corresponding covariance is

$$\tilde{X}(t_1) \approx \tilde{A}\tilde{X}(t_0)\tilde{A}^T \tag{21}$$

Errors in the state estimate, e, after the maneuver are

$$e(t_1) \approx e(t_0) + \begin{bmatrix} 0 \\ R^T \end{bmatrix}\delta y \tag{22}$$

where δy is the maneuver execution error derived in Ref. 7. From Eq. (22) it follows that the error covariance after the maneuver is

$$P(t_1) = P(t_0) + \begin{bmatrix} 0 & 0 \\ 0 & R^T Q R \end{bmatrix} \tag{23}$$

where Q is the covariance of the execution error. The elements of Q are given in Ref. 7.

III. Numerical Example

1980 Encke Slow Flyby Mission

A slow flyby of the comet Encke during its 1980 apparition was considered. This particular mission has been analyzed in some detail.[3-5] The performance of the navigation system is evaluated with respect to the accuracy with which it can deliver the spacecraft to the desired encounter conditions. The quantitive measure of navigation accuracy is the semimajor axis (SMAA) of the 0.997 probability position error ellipse in the impact plane. Navigation coast arcs ranging from 0-10 days in length were considered. The knowledge and delivery errors before and after the trim maneuver are given in Table 1 for various lengths of navigation coast. Delivery errors correspond to state errors mapped to encounter, and knowledge errors correspond to errors in the

Table 2 Statistical properties of the maneuver duration

Navigation coast length (days)	Mean maneuver duration (min)	Standard deviation (min)	$G(0.4)$	$G(0.8)$	$G(1.2)$
0	20.67	14.34	0.658	0.947	0.996
2	21.37	13.91	0.647	0.948	0.997
4	22.60	13.99	0.614	0.941	0.996
7	25.22	14.79	0.537	0.919	0.993
10	44.54	23.52	0.206	0.600	0.870

state estimate mapped to encounter. Because the maneuver is designed to remove all known position errors, the knowledge error prior to the maneuver represents the delivery accuracy possible with perfect guidance. The change in the knowledge error during the maneuver is casued by the execution error. For this analysis the thrust vector errors during the maneuver were assumed as follows: thrust vector pointing, 15 mrad; throttling, 10.0% of nominal thrust; and shut-off timing, 1 min. The statistical properties of the maneuver duration are given in Table 2. More detailed navigation results for this Encke mission are presented in Ref. 7.

IV. Conclusions

The coast arc strategy presented in Ref. 5 offers a means of effective terminal navigation in low-thrust flyby missions to small bodies. The analytical technique presented in this Note permits a more accurate statistical analysis of the trim maneuver in the coast arc strategy than is possible with the linear perturbation techniques employed previously. Changes in the thrust vector need no longer be assumed small. Instead, the trim maneuver may now be assumed to be performed at full throttle and in a direction which causes delivery errors to be eliminated while maneuver time is minimized.

References

[1] Jordan, J.F., "Orbit Determination by Powered Flight Space Vehicles on Deep Space Missions," *Journal of Spacecraft and Rockets,* Vol. 6, May 1969, pp. 545-550.

[2] McDanell, J.P., "Earth-Based Orbit Determination for Solar Electric Spacecraft with Application to a Comet Encke Rendezvous," AIAA Paper 73-174, Washington, D.C., 1973.

[3] Jacobson, R.A., McDanell, J.P., and Rinker, G.C., "Terminal Navigation for the 1980 Comet Encke Slow Flyby Mission," *Journal of Spacecraft and Rockets,* Vol. 11, Aug. 1974, pp. 590-596.

[4] Hong, P.E., Schults, G.L., and Boain, R.J., "System Design Impact of Guidance and Navigation Analysis for an SEP 1979 Encke Flyby," AIAA Paper 73-1061, Lake Tahoe, Nev., 1973.

[5] Jacobson, R.A., McDanell, J.P., and Rinker, G.C., "Use of Ballistic Arcs in Low Thrust Naviagtion," *Journal of Spacecraft and Rockets,* Vol. 12, March 1975, pp. 138-145.

[6] Lee, B.G. and Boain, R.J., "Propellent Requirements for Midcourse, Velocity Corrections," *Journal of Spacecraft and Rockets* Vol. 10, Dec. 1973, pp. 779-782.

[7] Rinker, G.C., Wood, L.J., and Jacobson, R.A., "Statistical Analysis of Trim Maneuvers in Low Thrust Interplanetary Navigation," AIAA Paper 75-85, Pasadena, Calif., 1975.